J Neuropathol Exp Neurol
Vol. 68, No. 12
December 2009
pp. 1256–1268

ORIGINAL ARTICLE

A Subpopulation of Rat Muscle Fibers Maintains an Assessable Excitation-Contraction Coupling Mechanism After Long-Standing Denervation Despite Lost Contractility

Roberta Squecco, PhD, Ugo Carraro, MD, Helmut Kern, MD, Amber Pond, PhD, Nicoletta Adami, MS, Donatella Biral, MS, Vincenzo Vindigni, MD, Simona Boncompagni, PhD, Tiziana Pietrangelo, MS, Gerardo Bosco, MD, Giorgio Fanò, PhD, Marina Marini, PhD, Provvidenza M. Abruzzo, MS, Elena Germinario, MS, Daniela Danieli-Betto, PhD, Feliciano Protasi, PhD, Fabio Francini, PhD, and Sandra Zampieri, PhD

Abstract

To define the time course and potential effects of electrical stimulation on permanently denervated muscle, we evaluated excitation-contraction coupling (ECC) of rat leg muscles during progression to long-term denervation by ultrastructural analysis, specific binding to dihydropyridine receptors, ryanodine receptor 1 (RYR-1), Ca^{2+} channels and extrusion Ca^{2+} pumps, gene transcription and translation of Ca^{2+}-handling proteins, and in vitro mechanical properties and electrophysiological analyses of sarcolemmal passive properties and L-type Ca^{2+} current (I_{Ca}) parameters. We found that in response to long-term denervation: 1) isolated muscle that is unable to twitch in vitro by electrical stimulation has very small myofibers but may show a slow caffeine contracture; 2) only roughly half of the muscle fibers with "voltage-dependent Ca^{2+} channel activity" are able to contract; 3) the ECC mechanisms are still present and, in part, functional; 4) ECC-related gene expression is upregulated; and 5) at any time point, there are muscle fibers that are more resistant than others to denervation atrophy and disorganization of the ECC apparatus. These results support the hypothesis that prolonged "resting" [Ca^{2+}] may drive progression of muscle atrophy to degeneration and that electrical stimulation–induced [Ca^{2+}] modulation may mimic the lost nerve influence, playing a key role in modifying the gene expression of denervated muscle. Hence, these data provide a potential molecular explanation for the muscle recovery that occurs in response to rehabilitation strategies developed based on empirical clinical observations.

Key Words: Excitation-contraction coupling, DHPR, RYR-1 Ca^{2+} channels, Gene expression, L-Type Ca^{2+} current, Long-term denervation, Sarcotubular system.

From the Interuniversitary Institute of Myology (RS, UC, NA, SB, TP, GB, GF, MM, PMA, EG, DD-B, FF, FP, SZ), Chieti, Italy; Department of Physiological Sciences (RS, FF), University of Florence, Florence, Italy; Laboratory of Translational Myology of the University of Padova Interdepartmental Research Center of Myology (UC, NA, VV, SZ), c/o Department of Biomedical Sciences, Padova, Italy; Italian CNR Institute of Neuroscience, University of Padova, Italy (UC, DB); Ludwig Boltzmann Institute of Electrostimulation and Physical Rehabilitation, Department of Physical Medicine (HK), Wilhelminenspital, Vienna, Austria; Department of Basic Medical Sciences (AP), School of Veterinary Medicine, Purdue University, West Lafayette, Indiana; Department of Basic and Applied Medical Sciences (SB, TP, GB, GF, FP), Centro Scienze dell'Invecchiamento (CeSI), University G. d'Annunzio, Chieti, Italy; Department of Histology, Embryology and Applied Biology (MM, PMA), University of Bologna, Italy; Department of Anatomy and Physiology (DD-B, EG), University of Padua, Italy; and Division of Rheumatology (SZ), Department of Clinical and Experimental Medicine, University of Padova, Italy.

Send correspondence and reprint requests to: Sandra Zampieri, PhD, Laboratory of Translational Myology of the University of Padova, Interdepartmental Research Center of Myology, c/o Department of Biomedical Sciences, Viale G. Colombo 3, I-35121 Padova, Italy; E-mail: sanzamp@unipd.it

This study was supported by the European Union Commission Shared Cost Project RISE (Contract No. QLG5-CT-2001-02191); the Austrian Ministry of Transport, Innovation and Technology "Impulsprogramm" Grant No. 805.353; research funds from the Ludwig Boltzmann Institute for Electrostimulation and Physical Rehabilitation at the Institute of Physical Medicine and Rehabilitation (Wilhelminenspital, Vienna, Austria); Italian C.N.R. funds and the Italian MIUR funds (ex60%) and PRIN 2004–2006 Program (Contract No. 2004061452-002) to Ugo Carraro; research funds from the Faculty of Sport Medicine to Feliciano Protasi; Research Grant No. 2004,0813 Ente Cassa di Risparmio di Firenze to Fabio Francini; and the USDA-CSREES Hatch Project No. IND076045 to Amber Pond.

INTRODUCTION

One of the effects of spinal cord injury (SCI) is rapid loss of contractile force and muscle mass. Atrophy of leg muscles is particularly severe when the injury destroys the lower motor neurons (LMNs) and, hence, the contacts between muscle and neurons. Within weeks after SCI, human muscles become unable to sustain tension during tetanic contractions induced by electrical stimulation (1–3). Within months after complete injury of the conus medullaris and cauda equina, the muscles are no longer excitable by commercially available electrical stimulators (4–6). This is because they have undergone severe disorganization of contractile elements (i.e. myofibrils) and of the excitation-contraction coupling (ECC) apparatuses. Finally, after several years of LMN denervation, muscle fibers are almost completely replaced by adipose and fibrous tissues (7, 8). This severe degeneration of muscle tissue does not occur in patients with

upper motor neuron lesions even 20 years after thoracic-level SCI (9).

We have demonstrated that the striking alterations of functional and structural properties of muscle fibers caused by the permanent lack of innervation in SCI patients can be prevented or reverted by functional electrical stimulation (FES) using custom-designed electrodes and stimulators developed in Vienna, Austria (8, 10–22). Previously, because long-term denervated muscles do not respond with twitch contraction even when they are stimulated by surface electrodes and commercial electrical stimulators, it was believed that FES was effective only when it was started early after a LMN lesion. Whether this lack of twitch response is the result of poor excitability or the disarrangement of contractile machinery is still a question that would require time course studies that for ethical reasons are difficult to perform in humans. Thus, it is important to have more detailed information on denervation-induced alterations that occur in ECC during progressive denervation.

The major components of ECC control are the L-type Ca^{2+} channels (also called *dihydropyridine receptors* [DHPRs]) localized in the transverse tubule (T tubule) membrane (23–25) and the Ca^{2+} release channels (also called *ryanodine receptors* [RYRs]) located in the sarcoplasmic reticulum (SR) (23, 26–28). A functional ECC system requires functional RYR Ca^{2+} release channels coupled with functional DHPR channels and T tubule integrity (29). A role for these structures in denervation-induced modifications occurring in muscle has been suggested both in muscle paralysis (8, 30) and in neurodegenerative diseases (31, 32).

Here, we report our observations from a rat model that has the advantage of undergoing progression from muscle atrophy to degeneration on a much shorter time scale than in humans, that is, weeks and months rather than years (7, 8, 33, 34). The denervation-induced alterations in the ECC apparatus were studied using multiple modalities before and after the denervated rat muscle lost in vivo surface electrical stimulation–induced contractility (i.e. 13–15 weeks after sciatectomy) and several months later when muscle fibers were still numerous but were severely atrophic and almost unable to contract in vitro. The results support the hypothesis that changes in intracellular calcium concentration ($[Ca^{2+}]i$) play a key role in modifying denervated muscle gene expression. Hence, they provide a potential mechanistic explanation for the muscle degeneration and recovery induced in LMN-denervated human muscles by an empirical FES strategy based on clinical observations.

MATERIALS AND METHODS

Denervation of Rat Leg Muscles

This research adhered to the Guiding Principles in the Care and Use of Animals of the American Physiological Society and was approved by the Padua and Florence Universities Ethics Committees. Male Wistar rats (weighing 150–200 g) were anesthetized using an intraperitoneal cocktail (ketamine hydrochloride 40 μg plus xylazine 20 μg/100 mg of body weight). The posterior tight areas were shaved and aseptically prepared using a povidone-iodine and 70% alcohol solution. Both right and left posterior legs were denervated by removal of a 2-cm portion of the sciatic nerve; the proximal stump near the trochanter muscles was tied. We performed sciatectomy on 25 rats and killed 5 rats per period (0, 3, 13, 26, and 44 weeks after sciatectomy) for all analyses except transmission electron microscopy (TEM) using an overdose of anesthetic. The leg muscles were immediately dissected. Loss of muscle mass (atrophy) was evaluated by weighing soleus, tibialis anterior (TA), and gastrocnemius muscles (Fig. 1). TEM was performed on muscles from rats (n = 12) treated similarly except that they were harvested at 9, 13, 18, and 36 weeks after sciatectomy.

TEM and Classification of Muscle Fibers

Dissected muscles were fixed in 0.2 mol/L sodium cacodylate buffer, pH 7.2, containing 3.5% glutaraldehyde for 2 hours, followed by buffer rinse and fixation for 1 hour in 1% osmium tetroxide. The specimens were rapidly dehydrated in graded ethanol and acetone, infiltrated with Epon-acetone (1:1) for 2 hours, and embedded in Epon. For T tubule staining, muscles were fixed in 0.1 mol/L sodium-cacodylate buffer (pH 7.2, 4°C) containing 3.5% glutaraldehyde and 75 mmol/L $CaCl_2$ for 1 to 2 hours. These specimens were then postfixed in a 2% OsO_4–0.8% $K_3Fe(CN)_6$ mixture for 1 to 2 hours followed by a rinse in 0.1 mol/L sodium cacodylate buffer with 75 mmol/L $CaCl_2$. The specimens were then dehydrated, infiltrated with Epon-acetone, and embedded as previously described. Ultrathin sections (~40 nm thick) and semithin sections (100 nm) were cut with a Leica Ultracut R (Leica Microsystem, Austria) using a Diatome diamond knife (Diatome Ltd CH-2501 Biel, Bern, Switzerland) and stained in 4% uranyl acetate and lead citrate. Stained sections were examined with an FP 505 Morgagni Series 268D electron microscope (Philips, Italy) at 60 kV equipped with a Megaview III digital camera and Soft Imaging System. Muscle fibers were examined in longitudinal sections; each muscle fiber was followed for as long as

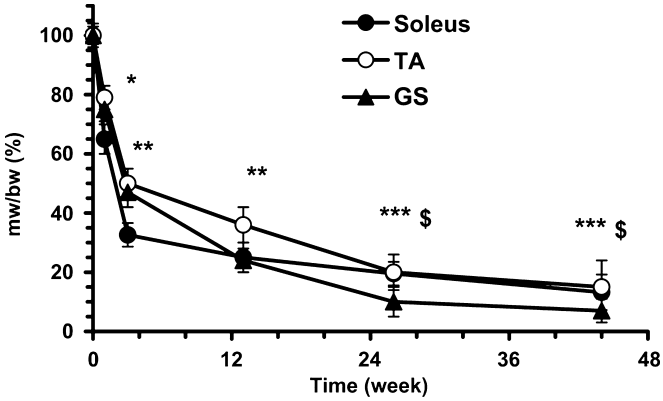

FIGURE 1. Denervation progressively reduces muscle weight–to–body weight ratio. Muscle weight–to–body weight ratios (mw/bw) of soleus, tibialis anterior (TA), and gastrocnemius (GS) muscles from rat legs at 0, 3, 13, 26, and 44 weeks after sciatectomy are expressed as percentage of the corresponding innervated control muscles. $^{**}p < 0.01$ and $^{***}p < 0.005$ compared with control; $^{\$}p < 0.05$ compared with 3-week–denervated muscles. N = 25 rats.

possible. All fibers visible in thin sections were analyzed and classified according to the level of structural integrity of the contractile apparatus, that is, presence or absence of pale-dark cross striations.

Cell-Free Analyses

The sarcolemmal fraction was purified from gastrocnemius muscles essentially as described by Gaillard et al (35); SR membranes were prepared as described by Renganathan (36). Membrane damage induced by lipid peroxidation activity of the intracellular antioxidant apparatus was determined as indicated by the Fulle group (37, 38). Measurement of extrusion Ca^{2+} pump activity was based on methods of Belia et al (39). Specific binding methodologies were used to measure the presence of DHPR and RYR-1 Ca^{2+} channels. In brief, Ca^{2+}-ATPase activity was measured using 50 μg of sample protein in a final volume of 1 mL of incubation medium containing 2.5 mmol/L adenosine triphosphate plus 10 μmol/L $CaCl_2$. For [^{3}H]ryanodine binding studies, SR vesicles were washed in binding buffer and centrifuged at 100,000 × *g* for 90 minutes before resuspension in binding buffer at a final concentration of 1 mg/mL. Aliquots (65 mg) of protein were incubated at 25°C in a final 250-mL volume of binding buffer containing 10 nmol/L [^{3}H]ryanodine for 120 minutes, then filtered with Whatman GF/C filters and washed with 6 volumes of ice-cold 10 mmol/L HEPES (pH 7.4) with 200 mmol/L KCl. The amount of bound [^{3}H]ryanodine was determined by liquid scintillation. For [^{3}H]PN200-110 binding assays, the DHPR concentration was determined using the radioligand [^{3}H]PN200-110. Sample protein (100 mg) was incubated in a final volume of 250 mL binding buffer in the presence of 1 nmol/L [^{3}H]PN200-110 for 1 hour at room temperature. After this, samples were filtered through Whatman GF/C filters and washed with 6 volumes of ice-cold washing buffer. Radioactivity was determined by liquid scintillation. Nonspecific [^{3}H]PN200-110 binding was assessed in the presence of 10 mmol/L unlabeled nifedipine.

Gene Expression by Real-Time Quantitative Polymerase Chain Reaction

Frozen TA muscles were reduced to powder using a sterilized ceramic mortar and pestle. Total RNA was isolated using TRIZOL (Invitrogen SRL, Milan, Italy) following manufacturer's instructions (40). RNA was not degraded, as assessed by evaluation of 28S and 18S band sharpness after denaturing gel electrophoresis. Samples were devoid of contaminating genomic DNA, as assessed by polymerase chain reaction (PCR) analysis performed with primers specific for the tubulin promoter. Reverse transcription was performed using the Omniscript Reverse Transcription Kit (Qiagen GmbH, Hilden, Germany). The primer sequences for the 7 genes studied and the housekeeping gene and the sizes of their amplification products are listed in Table 1. Primers were chosen at the 3′ end using the AMPLIFY free software; primers were designed to span an exon-exon junction whenever possible and were obtained from PROLIGO (Proligo, Paris, France). In preliminary PCR reactions, a melting curve analysis of the amplicons was run to check for possible nonspecific products; if they were present, different pairs of primers were used until the optimal combination was obtained. Real-time PCR was performed in an ABI PRISM 5700 real-time thermal cycler using the SYBR Green kit (Qiagen, Milan, Italy) and conventional methods. The housekeeping gene muscle creatine kinase (MCK) was used for normalization purposes because its expression is known to be unaffected by denervation (41, 42). All samples were devoid of contamination that would inhibit the PCR reactions as evidenced by the amplification efficiency of the MCK sequence which was approximately 95% ± 2% in all samples. For normalization, real-time PCR was initially run with MCK primers alone; the concentration of each sample was adjusted to match that of MCK cDNA. Subsequently, the differential expression of the other genes was evaluated using the $2^{-\Delta\Delta CT}$ comparison method (43), taking into account the amplification efficiency of each gene (44). At least 2 independent real-time PCR evaluations were carried out for each sample, and the results were averaged before calculating the means for control and each postdenervation time point. Because MCK mRNA is highly expressed, the value of 100 was arbitrarily assigned to its amount in about 10 ng of cDNA; the value for each gene was expressed by comparison with it. Data are expressed as mean ± SD. The 2-tailed Student *t*-test for unpaired observations was used to detect significant differences between control and denervated groups. The significance level was $p \leq 0.05$.

Protein Analysis

Tibialis anterior muscles from control and denervated rats were homogenized in 3% sodium dodecyl sulfate, 1 mmol/L ethylene glycol tetraacetic acid, boiled for 5 minutes and centrifuged at 900 × *g* for 15 minutes. For

TABLE 1. Primer Sequence and Amplicon Length of the Genes Studied by Real-Time PCR

Unigene Accession No.	Gene	Left Primer	Right Primer	Amplicon Length
Rn 10756	*MCK*	5′-GGCGTAAAGCTTATGGTGGA-3′	5′-CAAAGTCGGTTGGTTGGACT-3′	156
Rn 9417	*Sub1beta L channel*	5′-AGGACCTTGGATCTCCCCTA-3′	5′-TCTCTGGACCAGCTGTGATG	195
Rn 10305	*NCX2*	5′-TTTGTGGTCATTGCTGTGTG-3′	5′-AGATGCTCCAAGAGGCTGTG-3′	100
Rn 90982	*ATP2b4*	5′-ACCTCAACCTCATTCCATGC-3′	5′-GCTAATGTCAGGCCTCCTTG-3′	159
Rn 10111	*Cals2*	5′-GTTCCAAGAGGCAGCTGAAC-3′	5′-GACGTAGGGTGGGTCTTTGA-3′	211
Rn 98847	*Myh3*	5′-AGAGTCTGTGAAGGGCCTGA-3′	5′-CAGCCTGCCTCTTGTAGGAC-3′	146
Rn 10092	*Myh2*	5′-GAACAGAAGCGCAATGTTGA-3′	5′-CTTCCTCGGCTTGTCTCTTG-3′	169

The *MCK* gene was chosen for normalization purposes.

each sample, 200 μg of total protein aliquots were loaded onto a 10% sodium dodecyl sulfate-polyacrylamide gel, electrophoresed, and transferred to nitrocellulose. Immunostaining of blots was performed using the following primary antibodies: monoclonal antibody for SERCA1 (Affinity Bioreagents, Rockford, IL), polyclonal antibody for CS1 (Affinity Bioreagents, Golden, CO), and monoclonal antibody for RyR1 (Affinity Bioreagents); secondary antibodies were anti-mouse or anti-rabbit alkaline phosphatase-conjugated antibodies (SIGMA, Milan, Italy) (45).

In Vitro Muscle Mechanography

Isometric contractile properties of denervated soleus and extensor digitorum longus (EDL) muscles were investigated in vitro in a vertical muscle apparatus (300B, Aurora Scientific, Inc, Aurora, Canada) using PBS (pH 7.2–7.4) containing 30 μmol/L *d*-tubocurarine and the following (in mmol/L): 120 NaCl, 4.7 KCl, 2.5 $CaCl_2$, 3.15 $MgCl_2$, 1.3 NaH_2PO_4, 25 $NaHCO_3$, and 11 glucose; the solution was bubbled with 95% O_2–5% CO_2. Stimulation conditions and tension recordings were performed as previously described (46, 47). Muscle responses were recorded via an AT-MIO 16 A/D card, and data were analyzed by a LabView-based computer program (National Instruments, Austin, TX). In separate experiments, 30 mmol/L caffeine was added to the medium, and the ability to produce tension was analyzed.

Electrophysiology and Mechanical Response to Voltage on Isolated Muscle Fibers

Membrane potential was recorded in current-clamp condition by a microelectrode inserted into a muscle bundle fiber placed on a coverslip. The fibers were superfused at a rate of 1.8 mL min^{-1} with a bath solution containing (in mmol/L): 150 NaCl, 5 KCl, 2.5 $CaCl_2$, 1 $MgCl_2$, 10 D-glucose, and 10 HEPESA. The microelectrodes were filled with a solution containing (in mmol/L): 150 CsBr, 5 $MgCl_2$, 10 ethylene glycol tetraacetic acid, and 10 HEPES. These solutions were filtered through 0.22-μm pore filters, and the pH was titrated to 7.4 with NaOH and to 7.2 with TEA-OH for bath and pipette solutions, respectively. Microelectrodes were pulled using a micropipette vertical puller (Narishige PC-10 Tritech Research, Inc, Los Angeles, CA) from borosilicate glass (GC 150-15; Clark, Electromedical Instruments, Reading, UK). When filled, the resistance of the microelectrodes measured 8 to 10 MΩ. The passive properties of the fibers and L-type Ca^{2+} current (I_{Ca}) were evaluated with voltage-clamp in isolated fiber segments using the double Vaseline-gap method as previously described (48). The solutions used, data generation and acquisition, and mathematical and statistical analyses were as previously described (49, 50). For I_{Ca} recording, the fibers were held at −90 mV and then step pulses, 5 seconds long, from −80 to 40 mV were applied in 10-mV steps. The passive properties of the fibers were evaluated in voltage-clamp by applying a voltage pulse of ±10 mV from a holding potential of −80 mV. The resulting current decay could be fitted by the sum of 2 exponential functions. This function represents the time course of the surface and tubular membrane passive currents, I_S and I_T, respectively (51). The related time constants are $\tau s = R_s C_s$ and $\tau t = R_T C_T$, where R_s and R_T represent the resistances in parallel with C_s and C_T, respectively; C_s is the capacitance associated with the surface membrane and C_T is the capacitance associated with the tubular membrane. To allow comparison of test current recorded from different cells, I_{Ca} amplitudes and membrane resistance (Rm) were normalized to cell linear capacitance, Cm (where $Cm = C_s + C_T$ because Cm is an index of the total cell surface area assuming that membrane-specific capacitance is constant at 1 $\mu F/cm^2$). All experiments were performed at room temperature (20°C–23°C). The activation I-V relationship was described using the Boltzmann function: $I = Gmax (Vm-Vrev)/\{1 + \exp[(Vm-Va)/ka]\}$, where Gmax is the maximal conductance, Vm the membrane potential, Vrev is the reversal potential, Va is the voltage at halfway between Imax and 0, and ka is the constant that defines voltage sensitivity. I_{Ca} inactivation curves were evaluated using test pulses to 20 mV preceded by prepulses (1-second long, from −90 mV holding potential ranging from −80 to 50 mV, in 10-mV increments, pulse intervals 200 milliseconds). Inactivation curves were described using the Boltzmann function: $I = 1/\{1\text{-}\exp[(Vm-Vh)/kh]\}$, where Vh is the voltage at halfway between 1 and 0, and kh is the constant that defines voltage sensitivity.

For evaluation of mechanical response to voltage in the experiment with microelectrodes in current-clamp mode after the resting membrane potential evaluation, we applied a 5-second-long current step with a suitable intensity to produce a membrane potential of −80 ± 5 mV followed by a depolarizing current step to about 0/10 mV. The first current step reduced the inactivation state in the depolarized denervated fibers. The second step activated muscle contraction. This latter was estimated by microscope observation of a movement of the fiber near the stimulating microelectrodes.

Data are reported as mean ± the SEM or mean ± SD. One-way analysis of variance with repeated measures was used for multiple comparisons; a value of $p \leq 0.05$ was considered significant.

RESULTS

Muscle Weight–to–Body Weight Ratio of Denervated Muscles

As expected, denervated rat leg muscles showed a progressive decrease in muscle weight–to–body weight ratio (52, 53). This decrease was very marked in the first 3 to 13 weeks of denervation (Fig. 1). From 13 to 44 weeks, the decrease in muscle weight–to–body weight ratio progressed quite slowly; for soleus, the differences were not statistically significant when data at 13 weeks were compared with data at 44 weeks, indicating that the late loss of muscle mass is negligible.

Ultrastructural Analysis of Denervated Muscle

Denervated muscles analyzed by TEM showed significant alterations that were obvious at 9 weeks after sciatectomy and became more severe over time. The most evident denervation-induced alterations at the earlier time points were the grouping of mitochondria in longitudinal rows

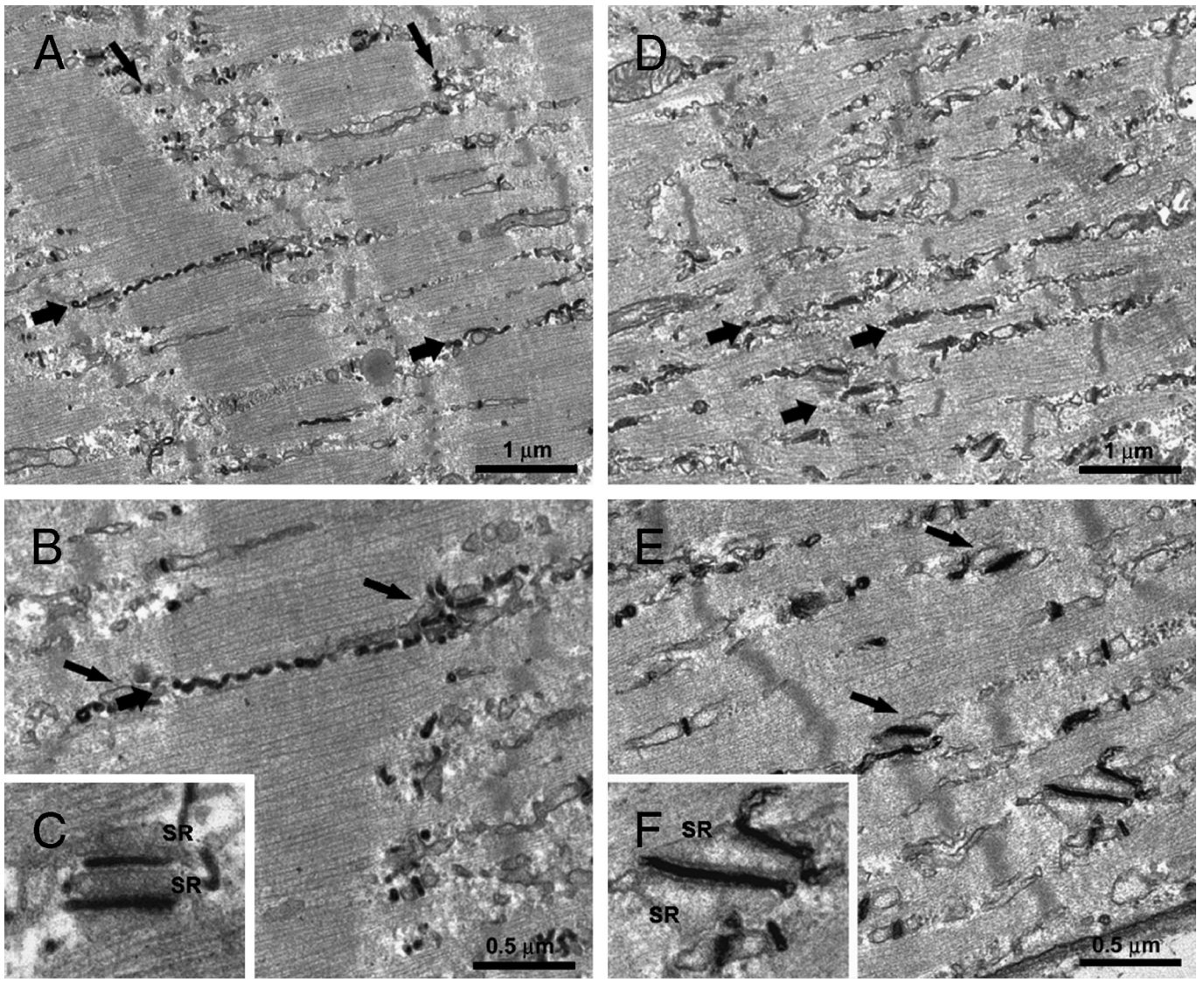

FIGURE 2. The sarcotubular system is severely compromised but maintains connection with the extracellular space. Soleus denervation results in severe alterations of the T tubular system, which tends to lose its transverse orientation (small black arrows) and its specific positioning at the I-A band transition **(A)**. The relative numbers of longitudinally oriented tubules (large black arrows) increase with longer times after denervation, (compare **[A]** and **[D]**, from 13 weeks and 18 weeks, respectively). Calcium release units in control muscle are almost exclusively transversally oriented and formed by 3 elements, whereas they are more variably oriented in denervated muscles (**[B]** and **[E]**, small black arrows, 13 weeks and 18 weeks, respectively) and formed by multiple elements (**[C]** and **[F]**). SR, sarcoplasmic reticulum.

(not shown) and initial disruption of the sarcotubular system (Fig. 2). With longer denervation periods, the muscles showed a progressive disruption of the myofibrillar apparatus with the consequent misorientation of Z lines and loss of striation. Widened and/or streaming Z lines, a common feature in a wide variety of muscle diseases (54), became more frequent. At 9 weeks after sciatectomy, most fibers (74%) still had cross striations, but at 18 weeks, most fibers (92%) lost this classic appearance, indicating a severe disarrangement of the contractile apparatus. Long-term–denervated fibers progressively displayed more severe changes. At 36 weeks, there was a complete disruption of the internal organization of myofibrils, disappearance of mitochondria, and extracellular spaces became enlarged and filled with adipose-infiltrated connective tissue with bundles of collagen fibers; such muscle fibers only weakly contract. Myofibrils and/or sarcomeres were quite rare after longer denervation periods, and mitochondria that were abundant early after denervation, although often abnormally clustered in longitudinal rows between myofibrils, also became increasingly rare.

The progressive disorganization of the contractile and metabolic machineries was accompanied by alterations affecting the membranous component of fibers, that is, T tubules and SR. T tubules, which were stained by a dark precipitate in 13-week–denervated fibers, tended to lose their normal transversal orientation (Fig. 2A) and their positioning

TABLE 2. Cell-Free Experiment Results on Functional Capacity of the Excitation-Contraction Coupling Apparatus

Determinations (Control vs Denervated)	Mean ± SE 13 Weeks	Mean ± SE 26 Weeks	n; p 13 Weeks	n; p 26 Weeks
SR lipid peroxidation, nmol MDA/mg protein	5.7 ± 0.08 vs 10.2 ± 0.35	n.d.	7; <0.01	—
Sarcolemmal lipid peroxidation, nmol MDA/mg protein	7.2 ± 0.18 vs 9.8 ± 0.11	n.d.	7; <0.05	—
SR Ca^{2+} ATPase, γPO_4^{-3}/min/mg/mL	28.2 ± 2.9 vs 7.5 ± 0.7	28.2 ± 2.9 vs 11.1 ± 0.9	9; <0.01	11; <0.01
Sarcolemmal Ca^{2+} ATPase, γPO_4^{-3}/min/mg/mL	11.8 ± 0.3 vs 7.4 ± 0.4	11.8 ± 0.3 vs 4.4 ± 0.5	6; <0.01	7; <0.01
[^{3}H]-ryanodine receptor binding, pmol/mg protein	8.7 ± 0.9 vs 4.8 ± 1.1	8.7 ± 0.9 vs 4.5 ± 0.8	7; <0.01	5; <0.01
[^{3}H]PN200-110 binding, pmol/mg protein	5.9 ± 0.3 vs 1.4 ± 0.2	5.9 ± 0.3 vs 1.3 ± 0.4	7; 0.01	7; <0.01

Data are mean ± SE of measurements carried out in samples derived from gastrocnemius muscles after either 13 or 26 weeks of denervation. n = number of animals tested. The 2-tailed Student *t*-test for unpaired observations was used to determine the statistical significance of observed differences.
n.d., not done; SR, sarcoplasmic reticulum.

at the I-A band transition of the sarcomere. The relative percentage of longitudinally oriented tubules increased with longer time postdenervation (Figs. 2A, D). The presence of the dark precipitate that had penetrated and stained the T tubular system provided direct evidence that this network, even if misoriented, was still connected to the surface membrane in long-term denervation (Fig. 2D).

Calcium release units (the junctions between T tubules and SR, which in adult muscle are usually transversally oriented and formed by 3 elements or "triads") were more variably oriented in denervated fibers, often longitudinal and/or oblique (Figs. 2B, E), and formed by multiple elements (pentads) (Figs. 2C, F). The SR components were also unusually shaped and, at longer denervation times, became incomplete and vesiculated.

Cell-Free Analyses

The SR controls the cytoplasmic concentration of Ca^{2+}. The release of Ca^{2+} from SR terminal cisternae is controlled by mechanical interactions between DHPRs located in the T tubule membrane and the SR Ca^{2+} release channels (RYR type 1). Alterations of the SR/T tubule membrane structure can affect this interaction and consequently the ECC mechanism. During denervation, there is a highly significant decrease of DHPR binding in denervated samples (Table 2). Table 2 also shows that 10 nmol/L [^{3}H]ryanodine binding to SR vesicles, derived from the muscles of denervated rats, exhibits decreased [^{3}H]ryanodine binding, thereby indicating a diminished capacity of Ca^{2+} channels to be maintained in the open state. If this is true, the concentration of free Ca^{2+} in the sarcoplasmic compartment was reduced after a medium denervation time; consequently, the activity of Ca^{2+} pumps able to remove Ca^{2+} from this site should be reduced. Indeed, in early denervation, there were rapid significant decreases in the activities of both the SR Ca^{2+} ATPase and the Ca^{2+} pump available in the sarcolemmal membrane (i.e. the Ca^{2+} ATPases that control intracellular Ca^{2+} homeostasis), which declined to 25% of normal values and remained at this value after long-term denervation. Denervated muscles also showed peroxidation of the membrane network, suggesting the presence of excess reactive oxygen species and, therefore, oxidative stress. Because under these experimental conditions ryanodine binds its receptor in proportion to its opening status, decreased binding in denervated muscle preparations can be ascribed not only to a decrease of functional RYR channels after 13 and 26 weeks of denervation, but also to a decreased SR Ca^{2+} channel opening status possibly caused by alteration of the muscle redox state.

Gene and Protein Expression

In normal rat leg muscles, mRNAs encoding Ca^{2+}-handling molecules were expressed at low or very low levels compared with mRNAs encoding myosin heavy chains (i.e. 4–6 orders of magnitude less). Using real-time PCR with

TABLE 3. Gene Expression of Calcium Channel Subunits, Calsequestrin 2, and Myosin Heavy Chains in Surgically Denervated Tibialis Anterior Muscle

Gene	Specific/Housekeeping Gene Expression (Fold Variation vs Control) Short-Term Denervation (15 days; n = 5)	Medium-Term Denervation (3 months; n = 4)	Long-Term Denervation (9 months; n = 4)
Subunit 1beta of L-type Ca^{2+} channels	11.8*	18.5*	5.3*
NCX2	36.3*	12.4*	6.8*
ATP2b4	5.6*	19.7*	11.4*
Calsequestrin 2	4.6*	13.9*	5.3*
Myh3-Embryonic Myosin Heavy Chain	NE	170.4*	57.4*
Myh2A/2X-Fast Myosin Heavy Chain	3.6*	5.0*	5.3*

The expression of specific genes (mRNA content) was normalized to that of the housekeeping gene, *MCK*. The fold variation of specific gene expression in denervated tibialis anterior (TA) muscle compared with control intact TA are shown (n = 6).
*Denotes statistical significance of denervated muscle mRNA measurement compared with that of control intact muscle ($p \leq 0.05$ by Student *t*-test).
NE, not evaluated.

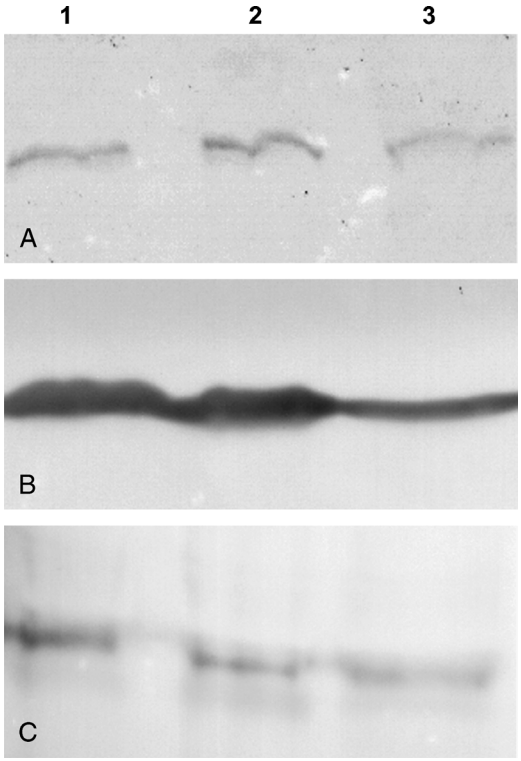

FIGURE 3. Immunoblots of ryanodine receptor (RyR) **(A)**, calsequestrin **(B),** and sarco(endo)plasmic reticulum Ca^{2+}-ATPase (SERCA) **(C)** using 200 μg protein aliquots of total homogenate of normal adult rat muscle [1], and 13 weeks [2] and 44 weeks [3] postdenervated rat muscles. Calsequestrin **(B)**, a sarcoplasmic Ca^{2+}-binding protein is decreased in the total homogenate of long-term–denervated muscle. Measurable amounts of calcium release and reuptake proteins, RYR **(A)** and SERCA **(C)**, respectively, are also detected.

concentrated cDNA (100 ng/μL), we tracked changes in expression; no mRNA encoding the three Ca^{2+} channels/transporters examined could be detected when rat liver cDNA was substituted for muscle cDNA in the reaction. Because liver is a nonexcitable tissue, it is a suitable negative control.

We determined amounts of mRNA encoding: 1) the β1 subunit of the Ca^{2+} L-type channels; 2) a sodium-calcium exchanger, NCX2; 3) a calcium ATPase transporter, ATP2b4; and 4) calsequestrin2, a protein involved in the storage of Ca^{2+} ions in the endoplasmic reticulum. Remarkably, all the examined mRNAs displayed significant increases relative to control intact muscle in denervated tissue (Table 3). The relative increases, however, were less in long-term–denervated muscle.

Consistent with the progressive shift toward intermediated/fast-type fibers known to occur with denervation, fast-type IIA/IIX myosin heavy chain mRNA was also overexpressed in denervated muscles. Remarkably, the relative increase progressed more quickly in the early postdenervation phases than in later ones. Gene expression of embryonic myosin heavy chain was also greatly increased, confirming that there are attempts for regenerative processes even in long-term–denervated muscle (33, 55–58).

Calsequestrin, an SR $Ca^{(2+)}$-binding protein that modulates RyR1 function, was found to be present in total homogenates of leg muscle of long-term–sciatectomized rats, together with measurable amounts of calcium release and reuptake proteins (RYR and SERCA, respectively) (Fig. 3).

In Vitro Contractility of Isolated Muscle

Maximum tetanic tension by in vitro electrostimulation in short-term–denervated EDL and soleus muscles was reduced to about 50% and 32%, respectively, compared with controls; it was dramatically reduced in long-term–denervated muscles to about 16% and 11% of controls, respectively. Neither EDL nor soleus muscles responded to stimulation frequencies higher than 40 Hz (data not shown). At the longest postdenervation time studied, several muscles were also unable to deliver electrostimulated twitch tension, but administration of caffeine evoked a contracture in 3 of 4 of the 44-week–denervated electrically unexcitable EDL muscles (Fig. 4). Thus, the ryanodine-dependent internal Ca^{2+} release and storage systems were still present in these muscles, as shown in Figure 3.

Electrophysiology and Mechanical Response to Voltage of Isolated Muscle Fibers

The measured mean diameters of the myofibers used for the electrophysiological recording were comparable to those determined by histological morphometric analysis (Fig. 5A). To evaluate the progressive modifications occurring in membranes of denervated muscle fibers, we first measured the resting membrane potential (Vm) in current clamp conditions (Tables 4 and 5). The values in control soleus fibers were about −86 mV. Medium-term–denervated fibers showed a progressive membrane depolarization; a depolarized state remained quite stable (at about −55 mV) through long-term denervation (Fig. 5B). A similar denervation time dependence was observed for the passive properties of the sarcolemma evaluated in voltage-clamp conditions. The membrane resistance normalized to the surface membrane capacitance, RmCm, decreased progressively from 6,000 ΩμF in control to 3,200 ΩμF (~55%) after 13-week denervation and did not significantly change thereafter (Fig. 5C). The analysis of the passive properties of the fibers (assessed in voltage-clamp by applying a voltage pulse of ±10 mV from a holding potential of −80 mV) showed that the current decay could be fitted by the sum of 2 exponential functions that represented the capacitance associated

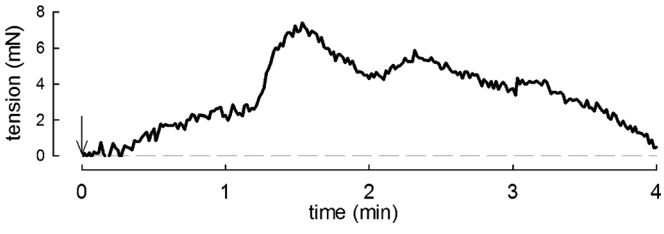

FIGURE 4. Caffeine contracture in denervated extensor digitorum longus (EDL) muscle. Representative record of caffeine contracture in long-term–denervated rat EDL muscle. Addition of 30 mmol/L caffeine is indicated by an arrow.

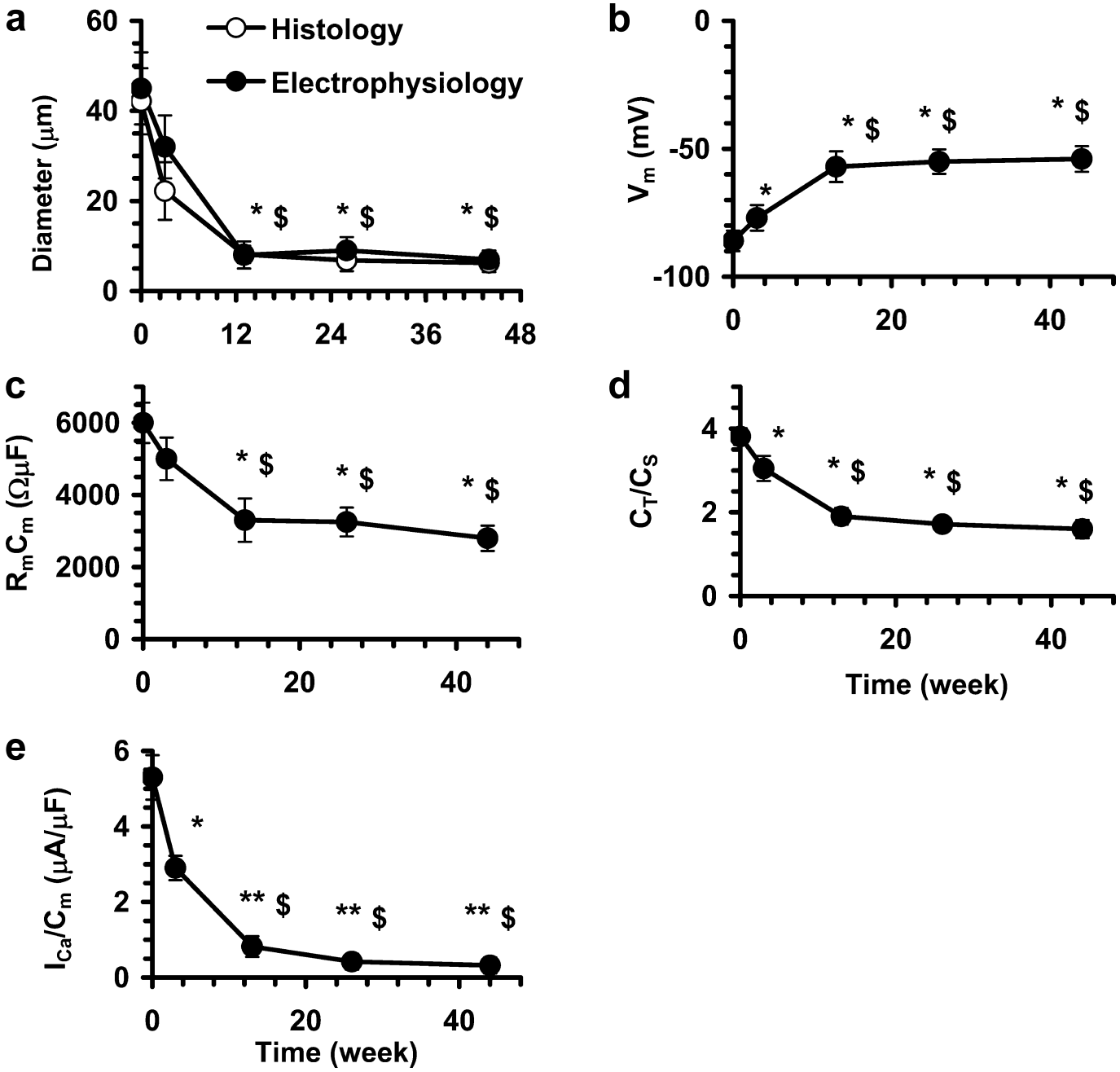

FIGURE 5. Soleus denervation progressively reduces, but does not abrogate, resting membrane potential, passive properties of sarcolemma, and L-type Ca^{2+} current (I_{Ca}). **(A)** Mean fiber diameters evaluated by histology compared with those used for electrophysiological in vitro analyses. **(B)** Resting membrane potential evaluated in current clamp. **(C)** Membrane resistance (R_m) normalized for the total membrane capacitance (C_m). **(D)** Tubular capacitance (C_T)–to–surface capacitance (C_s) ratio. **(E)** Normalized I_{Ca} evaluated at the peak current elicited by voltage pulses at 10 mV. Values for electrophysiological experiments in control (0), and at 3, 13, 26, and 44 weeks after sciatectomy are shown. Numbers of muscle fibers are reported in Table 5. Significant changes at *$p < 0.01$ and **$p < 0.005$ compared with controls. Significant differences at $^{\$}p < 0.05$ compared with 3-week–denervated soleus muscles.

with the surface membrane, C_s, and the tubular membrane, C_T. The extension of the tubular membrane surface changed with respect to that of the sarcolemmal surface as evaluated by the ratio C_T/C_s (Fig. 5C). The C_T/C_s ratio markedly decreased in the first 13-week postdenervation (from 3.8 in control to 1.9 [~50%] in 13-week postdenervation fibers) and remained stable thereafter (1.7 and 1.6, respectively, in 26- and 44-week–denervated fibers).

Comparable changes in fiber diameter, resting membrane potential, specific membrane resistance, and C_T/C_s

TABLE 4. Soleus Denervation Determines Reduction of Normalized Maximal Conductance (G_{max}/C_m) and Voltage Shift of Half Activation, Half Inactivation, and Reversal Potential Values

Weeks After Sciatectomy (No. Muscles Studied)	N (%)	G_{max}/C_m, nS/mF	V_a, mV	k_a, mV	V_{rev}, mV	V_h, mV	k_h, mV
0 (4)	18 (100)	120.2 ± 12.2	−9.1 ± 2.1	12.9 ± 2.1	56.2 ± 6.1	−42 ± 4.5	4.5 ± 1.4
3 (4)	13 (87)	93.5 ± 10.3*	−1.9 ± 1.6*	12.8 ± 2.4	47.8 ± 5.4*	−45 ± 5.5	5.2 ± 1.8*
13 (4)	10 (33)	42.2 ± 6.2†	4.8 ± 2.7†	12.7 ± 2.5	36.1 ± 4.2†	−50 ± 5.0*	8.8 ± 3.3†
26 (5)	6 (24)	31.5 ± 8.3†	6.9 ± 3.1†	12.6 ± 2.6	35.8 ± 4.3†	−52 ± 4.5*	9.1 ± 3.4†
44 (6)	6 (16)	18.1 ± 8.6†‡	7.8 ± 3.1†	12.6 ± 2.5	35.2 ± 4.4†	−53 ± 5.0*	9.7 ± 4.3†

Boltzmann parameters for I_{Ca} activation and inactivation in control and denervated soleus fibers and in muscle 26 weeks after sciatectomy and spontaneous reinnervation. n = number of fibers investigated; the percentages within parentheses indicate the number of fibers within the population of excitable cells that continued to conduct calcium current at the indicated time after sciatectomy.

Significant differences from control, *$p < 0.05$, †$p < 0.01$; ‡$p < 0.05$ compared with 13- and 14-week samples.

ratio were observed for TA fibers (Table 5). Notably, these parameters in TA at 26 and 44 weeks postdenervation were reduced compared with control muscle ($p < 0.01$), but there were no significant differences between them (Table 4). Representative normalized L-type current (I_{Ca} density, I_{Ca}/C_m) traces in control and denervated soleus specimens are shown in Figure 6. The numbers of fibers able to conduct I_{Ca} in response to electrical stimulation at any voltage used decreased progressively in denervated soleus muscle, but the reduction was more evident during the first 13 weeks after sciatectomy, reaching 33% of the total fibers investigated. The numbers of fibers able to conduct I_{Ca} decreased further with time, but at a slower rate, reaching 24% and 16% of controls in 26- and 44-week–denervated muscles, respectively (Table 5, second column). The previously described changes in fiber diameter, Vm, RmCm, and C_T/C_s (Figs. 6A–D) were paralleled by those observed for I_{Ca} density evaluated at the peak height (Figs. 6E, F) and Boltzmann parameters (Fig. 6G; Table 5). These changes were established more quickly up to 13-week denervation and at a slower pace in long-term–denervated fibers. The decreased I_{Ca} density and G_{max}/C_m suggested a reduced number of functional L-type Ca^{2+} channels in fibers able to conduct I_{Ca}. Moreover, the Boltzmann parameter changes evidenced a progressive alteration of I_{Ca} kinetics, being positively shifted 17 mV at 44 weeks with Vrev negatively shifted 21 mV at 44 weeks (Fig. 6G; Table 5). The observed voltage shift of Vrev together with the reduced RmCm value could be the result of an increase in intracellular Ca^{2+} concentration owing to a more leaky sarcolemma. Notably, denervated fibers showed faster kinetics: the time to peak at 10 mV was 320 ± 40 milliseconds in control and decreased to 256 ± 36 milliseconds in 3-week–denervated fibers and 138 ± 16 ms in 13- to 44-week–denervated fibers. The half decay of I_{Ca} evaluated at 40 mV was 1.1 seconds in control and decreased to 0.4 seconds in 13- to 44-week–denervated fibers.

We analyzed I_{Ca} inactivation in parallel experiments. Our results showed that denervation produced a shift toward more negative potentials of Vh (17 mV at 44 weeks) and an increase of k_h (from 4.5 in innervated to 9.7 in 44-week–denervated muscle; Fig. 6G; Table 5) with a similar time dependence. Accordingly, the changes in the activation and inactivation of Boltzmann parameters determined a reduction in the voltage window in which I_{Ca} can be elicited. At the depolarized membrane potential typical of the 44-week–denervated fibers, Ca^{2+} channels were inactivated (closed) about 40%. Therefore, the depolarized state of the membrane observed in long-term denervated fibers could be another factor that strongly reduced the amount of I_{Ca} in vivo. Comparable changes for resting membrane potential, passive properties of sarcolemma, and I_{Ca} density were observed for TA fibers (Table 5).

The presence of a residual contractility in isolated denervated fibers was tested in the experiments performed with microelectrodes in current clamp mode after the resting membrane potential evaluation. All the control fibers from the innervated muscles showed sarcomeric contraction, whereas in denervated soleus and TA fibers, the percentage of contractile fibers dropped drastically, with only 8% and 5% of soleus fibers and 8% and 3% of TA fibers contracted after 16 and 44 weeks of denervation, respectively. The percentage of fibers able to respond to electrical stimulation was less than those expressing I_{Ca} current (24% and 16%, Table 2), confirming that the denervation-induced modifications affected the sarcomeric structure and functionality more than Ca^{2+} channels.

DISCUSSION

In the rat model, permanently denervated muscles undergo 3 stages of alteration. Up to the fourth week of denervation, there is rapid atrophy accompanied by an increase of chronaxie that reaches a stable level of approximately 20 milliseconds. From 4 to 13 weeks after denervation, there is a period of slow progressive atrophy during which no significant

TABLE 5. Effects of Denervation on Tibialis Anterior Fiber Diameter, Resting Membrane Potential, Membrane Resistance, C_T/C_s Ratio, and I_{Ca}

	Diameter, μm	Resting Membrane Potential, mV	Rm, Ωcm²	CT/Cs	I_{Ca} (μA/μF)
Control	80 ± 6	−80 ± 11	5,800 ± 600	5.1 ± 2	6.4 ± 2
26 Weeks	20 ± 4	−40 ± 8	3,000 ± 500	2.6 ± 2	1.1 ± 2
44 Weeks	19 ± 5	−40 ± 8	2,900 ± 500	2.5 ± 3	0.9 ± 1

Data are from 8 to 22 fibers from 5 to 6 muscles.

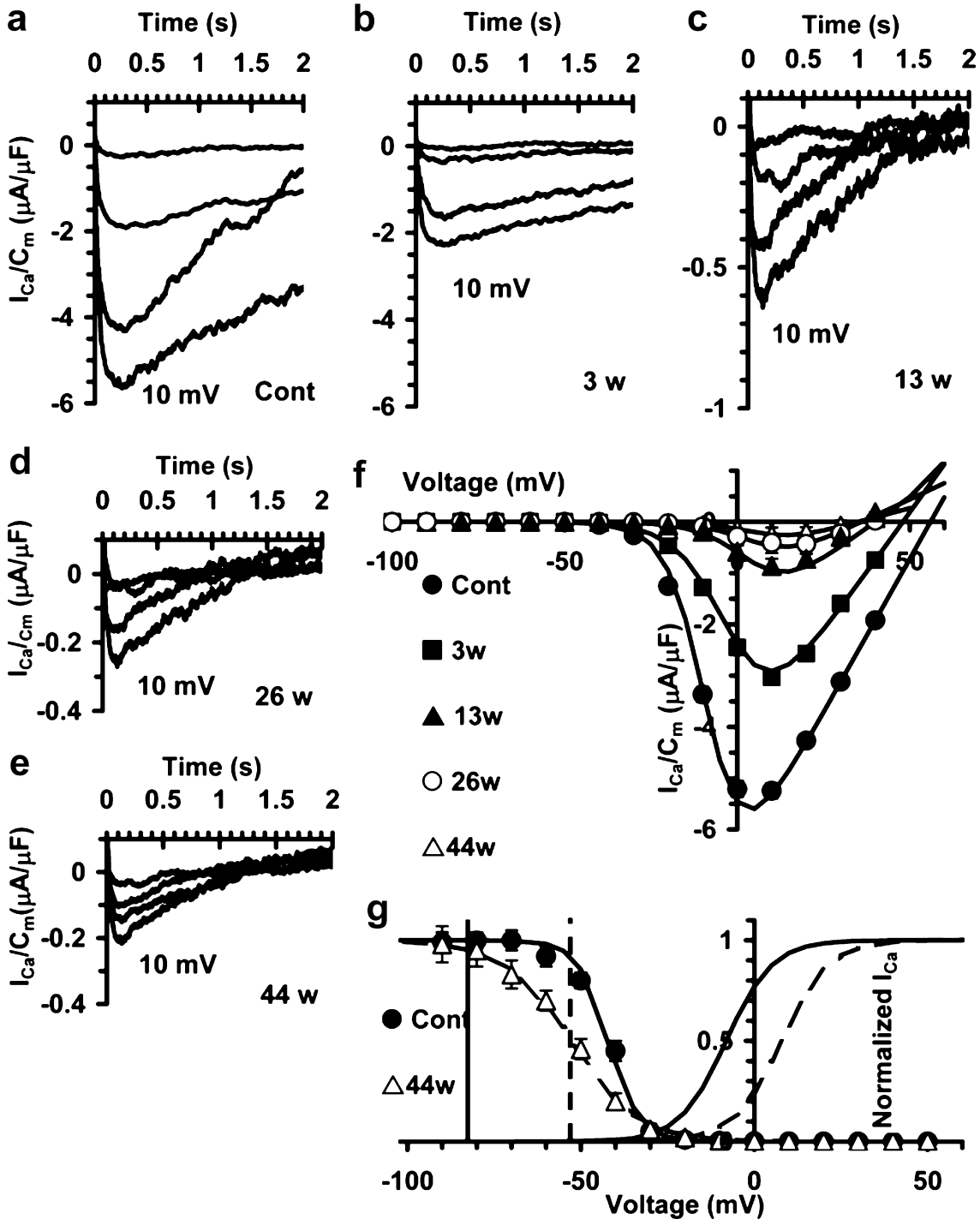

FIGURE 6. Long-term denervation in soleus muscle reduces L-type Ca^{2+} current (I_{Ca}) size and changes its kinetics. Representative normalized current traces recorded in single soleus muscle fibers in voltage-clamp elicited by voltage pulses from −80 to 40 mV in 10-mV increments from a holding potential of −90 mV in control **(A)**, 3 **(B)**, 13 **(C)**, 26 **(D)**, and 44 **(E)** weeks after denervation; for clarity, only current traces at −60, −20, 10, and 40 mV are shown. **(F)** Normalized I_{Ca} evaluated at the current peak versus membrane potential plots. Denervation decreases I_{Ca}. Related Boltzmann parameters are presented in Table 5. **(G)** Boltzmann curves for activation are obtained from data in **(F)**. Inactivation data are obtained using a test pulse to 20 mV preceded by prepulses (1-second long, ranging from −80 to 50 mV in 10-mV increments; pulse intervals 500 milliseconds). For clarity, only curves evaluated in control and 44-week–denervated fibers are shown. The Boltzmann parameters for all fibers investigated are listed in Table 5. Vertical lines indicate the resting membrane potential for control (continuous line) and 44-week (dashed line)–denervated fibers.

change in chronaxie occurs. From 26 weeks onward, the sizes of the severely atrophic muscle fibers remain stable, whereas chronaxie increases to an infinite value as a re-sult of poor stimulation-induced contractility. Meanwhile, myofibers decrease in number and fibrosis increases (33, 53, 59). In response to electrical stimulation (1) or caffeine treatment (Fig. 4), however, long-term–denervated muscles maintain residual contractile activity that can be assessed when isolated tendons or muscles are secured to appropriate transducers.

In agreement with histochemical analyses (53, 55, 60), our TEM evidence of mitochondrial decrease and misplacement suggests a shortage of energy metabolism that may contribute to dysfunction and impairment of ion channels and Ca^{2+} pumps. Indeed, muscle fiber ECC is minimally damaged before 13 weeks of denervation as the T tubule system remains connected with the extracellular space. These characteristics are similar to those described after denervation of developing rat muscles (61) and muscles regenerating in the permanent absence of the nerve (45, 62). On the other hand, our TEM images show that T tubules progressively lose their normal transverse orientation and position at the I-A band transition of the sarcomere from 18 weeks of denervation onward. The presence of the dark precipitate, which had penetrated and stained the T tubular system, however, indicates that the network remains connected to the surface membrane. These observations are in agreement with our recent data in denevated rabbit muscles (10, 63) and previous data on long-term–denervated human muscle (7, 11).

The decreases of DHPR and 10 nmol/L [^{3}H]ryanodine binding to SR vesicles in denervated muscles indicate that the molecular components and major ECC components of T tubule and SR systems are modified by denervation at the molecular/functional levels, suggesting a diminished capacity of Ca^{2+} channels to be maintained in the open state. Furthermore, the SR Ca^{2+} ATPase and the Ca^{2+} extrusion pump of the sarcolemma, which control intracellular Ca^{2+} homeostasis, exhibit a significant decrease in activity. On the other hand, the ATPase activity associated with SR membranes, which rapidly decreases to 25% of its normal value, does not decrease further during long-term denervation. Similarly, long-term–denervated muscles that are electrically unexcitable in vitro respond with a slow contracture in the presence of caffeine, confirming that at least a subset of long-term–denervated muscle fibers can release enough Ca^{2+} from the SR to invoke activation of the residual contractile proteins. This may be the result of weak contractions of all myofibers or of a subpopulation more resistant to denervation atrophy (64). As indicated by binding assays, Western blots and single-fiber electrophysiological analyses, the ryanodine-dependent internal Ca^{2+} release, reuptake, and storage systems were still present in the muscle fibers.

We found that the long-term–denervated rat muscle maintains L-type Ca^{2+} current longer than it maintains functional contractile machineries. That is, despite the decrease in functionality, density, and correct coupling of DHPR and RyR channels, some residual I_{Ca} activity remains in the long-term as indicated by real-time PCR, Western blots, and electrophysiological data. We present, for the first time, an in vitro electrophysiological analysis of single rat muscle fibers after long-term denervation. This is novel because the expectation was that the muscle fiber would basically disappear from permanently denervated muscle and that the increase in intramuscular fibrous tissue would hinder single analysis of residual muscle fibers. The electrophysiological analysis suggests that the loss of tubular surface area is more marked than that of membrane surface area and that the tubular system is not completely lost.

The reduced values of RmCm and the depolarized resting membrane potential in denervated fibers suggest a leaky sarcolemma and an increase of intracellular Ca^{2+} concentration; this was confirmed by the shift in Vrev of I_{Ca} toward a more negative potential. This may be a starting mechanism that reduces membrane excitability and the efficacy of electrical stimulation in short-term– and, to a greater degree, in long-term–denervated muscles. Indeed, this may explain why commercial electrical stimulators are unable to elicit tetanic contractions of long-term–denervated human muscles and why twitch contractions need extremely long pulses (more that 150 milliseconds) and high voltages to occur (7, 8, 11–22). The shift toward more positive potentials of I_{Ca} that we observed in long-term–denervated muscle indicates an increased number of uncoupled DHPRs (65). An increased number of DHPRs unlinked with RYRs and fast activation kinetics of I_{Ca} were also observed in a subset of skeletal muscle fibers of old mice (66).

The depolarized state of the denervated rat fiber is in agreement with the reduced action potential conduction velocity observed in human long-term–denervated muscles (67, 68). Reduced resting Rm together with the reduced muscle fiber diameter could explain the reduced excitability found in muscle of SCI patients as increased values of chronaxie and rheobase. The presence of functional voltage-dependent L-type Ca^{2+} channels may allow an influx of external Ca^{2+} that activates Ca^{2+}-dependent signaling pathways (e.g. calcineurin) to the nucleus, thus inducing the expression of muscle-specific proteins, increasing the muscle mass and restoring the metabolic and contractile machinery (69–71). The role of Ca^{2+} influx is corroborated by data revealing that in long-term–denervated muscle fibers, there is both an increased sensitivity of L-type Ca^{2+} channel to passive mechanical stretch (72) and a greater expression of stretch-activated channels (73).

We also present the first convincing evidence of increased expression of Ca^{2+}-handling genes in long-term–denervated muscles. Whether this mRNA upregulation leads to the synthesis of all of the respective functional proteins is an open issue, but immunoblots suggest that muscle fibers, although unable to respond to high-current stimulation, maintain the proteins that would be important in late reinnervation, albeit in lesser amounts. This upregulation of mRNAs encoding these Ca^{2+}-handling proteins in long-term–denervated muscle may represent a compensatory reaction to the reduction/absence of muscle action potentials and/or may be related to a second cell-based mechanism, that is, myoblast proliferation–dependent regenerative processes. In support of this, Carraro et al (57) showed that the hemidiaphragm had ultrastructural and molecular evidence of muscle fiber regeneration after long-term phrenectomy and also that satellite cell proliferation

and differentiation to adult muscle fibers could be repeatedly induced in permanently denervated leg muscles (58). These results were confirmed by others (1, 41, 42, 56, 74, 75) and by us in rat (55, 76) and in human long-term–denervated muscles (7, 8, 12). The evidence that a subpopulation of long-term–denervated muscle fibers (approximately 5% of those present 9 months after sciatectomy) are still able to respond with contraction to electrical stimulation may be simply the compound result of sparsely repeated muscle regeneration events; this is still unresolved. Nonetheless, we have demonstrated that a larger percentage (at least 15%) of long-term–denervated fibers still conduct voltage-dependent (I_{Ca}) currents and that all the long-term–denervated muscle fibers maintain a resting membrane potential, although at the lower level of the nonexcitable cells.

The present results are consistent with our previous observations that LMN-denervated human muscles have few damaged ECC and myofibrillar apparatuses and respond with weak tetanic contraction to direct electrical stimulation when examined after 9 months or less from SCI; they need very long (i.e. more than 150 milliseconds) impulses to perform twitch contractions when examined more than 18 months from SCI (15). After months of twitch training (8, 13–17), and thus of [Ca^{2+}] transients, the restored tetanic contractility could improve the synthesis/degradation balance of myofibrillar proteins. Altogether, our results support the hypothesis that electrical stimulation–induced changes in [Ca^{2+}] may mimic lost nerve influence and play a key role in modifying denervated muscle gene expression. Hence, our work provides a potential molecular explanation of the muscle recovery that occurs in response to the rehabilitation strategy of home-based FES in humans (8, 13–17, 20), which was developed as a result of empirical clinical observations (77).

ACKNOWLEDGMENTS

The authors thank V. Gobbo for microscopy and preparation of figures and G. Valle for expert support in the Western blots of Ca^{2+}-handling proteins.

REFERENCES

1. Al-Amood WS, Lewis DM, Schmalbruch H. Effects of chronic electrical stimulation on contractile properties of long-term denervated rat skeletal muscle. J Physiol 1991;441:243–56
2. Dulhunty AF, Gage PW. Excitation-contraction coupling and charge movement in denervated rat extensor digitorum longus and soleus muscle. J Physiol 1985;358:75–89
3. Kobayashi J, Mackinnon SE, Watanabe O. The effect of duration of muscle denervation on functional recovery in the rat model. Muscle Nerve 1997;20:858–66
4. Harrison D. Current trends in the treatment of established unilateral facial palsy. In: Karcher E, ed. *Functional Surgery of the Head and Neck*. Graz, Austria: RM Druck &Verlagsgesellschaft; 1989:9–16
5. Nightingale EJ, Raymond J, Middleton JW, et al. Benefits of FES gait in a spinal cord injured population. Spinal Cord 2007;45:646–57
6. Sunderland S. *Nerve and Nerve Injuries*. 2nd Ed. Edinburgh, Scotland: Churchill-Livingston; 1978
7. Rossini K, Zanin ME, Podhorska-Okolow M, et al. To stage and quantify regenerative myogenesis in human long-term permanent denervated muscle. Basic Appl Myol 2002;12:277–86
8. Kern H, Boncompagni S, Rossini K, et al. Long-term denervation in humans causes degeneration of both contractile and excitation-contraction coupling apparatus that can be reversed by functional electrical stimulation (FES). A role for myofiber regerenation? J Neuropathol Exp Neurol 2004;63:919–31
9. Kern H, Hofer C, Mödlin M, et al. Stable muscle atrophy in long-term paraplegics with complete upper motor neuron lesion from 3- to 20-year SCI. Spinal Cord 2008;46:293–94
10. Ashley Z, Salmons S, Boncompagni S, et al. Effects of chronic electrical stimulation on long-term denervated muscles of the rabbit hind limb. J Muscle Res Cell Motil 2007;28:203–17
11. Boncompagni S, Kern H, Rossini K, et al. Structural differentiation of skeletal muscle fibres in absence of innervation in humans. Proc Natl Acad Sci U S A 2007;104:19339–44
12. Carraro U, Rossini K, Mayr W, et al. Muscle fiber regeneration in human permanent lower motoneuron denervation: Relevance to safety and effectiveness of FES-training, which induces muscle recovery in SCI subjects. Artif Organs 2005;29:187–91
13. Hofer C, Mayr W, Stöhr H, et al. A stimulator for functional activation of denervated muscles. Artif Organs 2002;26:276–79
14. Kern H, Carraro U. Translational myology focus on clinical challenges of functional electrical stimulation of denervated muscle. Basic Appl Myol 2008;18:37–100 [http://www.bio.unipd.it/bam/bam.html]
15. Kern H, Carraro U, Adami N, et al. One year of home-based functional electrical stimulation (FES) in complete lower motor neuron paraplegia: Recovery of tetanic contractility drives the structural improvements of denervated muscle. Neurol Res 2009, In press
16. Kern H, Hofer C, Mayr W. Protocols for clinical work package of the European project rise. Basic Appl Myol 2008;18:39–44 [http://www.bio.unipd.it/bam/bam.html]
17. Kern H, Hofer C, Mödlin M. Denervated muscles in humans: Limitations and problems of currently used functional electrical stimulation training protocols. Artif Organs 2002;26:216–18
18. Kern H, Hofer C, Strohhofer M, et al. Standing up with denervated muscles in humans using functional electrical stimulation. Artif Organs 1999;23:447–52
19. Kern H, Rossini K, Carraro U, et al. Muscle biopsies show that FES of denervated muscles reverses human muscle degeneration from permanent spinal motoneuron lesion. J Rehabil Res Dev 2005;42:43–53
20. Kern H, Salmons S, Mayr W, et al. Recovery of long-term denervated human muscles induced by electrical stimulation. Muscle Nerve 2005;31:98–101
21. Mayr W, Bijak M, Rafolt D, et al. Basic design and construction of the Vienna FES implants: Existing solutions and prospects for new generations of implants. Med Eng Phys 2001;23:53–60
22. Mödlin M, Forstner C, Hofer C. Electrical stimulation of denervated muscles: First results of a clinical study. Artif Organs 2005;29:203–6
23. Flucher BE, Morton ME, Froehner SC, et al. Localization of the alpha 1 and alpha 2 subunits of the dihydropyridine receptor and ankyrin in skeletal muscle triads. Neuron 1990;5:339–51
24. Melzer W, Herrmann-Frank A, Liittgau HCh. The role of Ca^{2+} ions in excitation-contraction coupling of skeletal muscle fibres. Biochim Biophys Acta 1995;1241:59–116
25. Rios E, Brum G. Involvement of dihydropyridine receptors in excitation-contraction coupling in skeletal muscle. Nature 1987;325:717–20
26. Inui M, Saito A, Fleischer S. Isolation of the ryanodine receptor from cardiac sarcoplasmic reticulum and identity with the feet structures. J Biol Chem 1987;262:15637–42
27. Lai FA, Erickson HP, Rousseau E, et al. Purification and reconstitution of the calcium release channel from skeletal muscle. Nature 1988;331:315–19
28. Block BA, Imagawa T, Campbell KP, et al. Structural evidence for direct interaction between the molecular components of the transverse tubule/sarcoplasmic reticulum junction in skeletal muscle. J Cell Biol 1988;107:2587–600
29. Sanger JW, Sanger JM, Franzini-Armstrong C. Assembly of the skeletal muscle cell. In: Engel AG, Franzini-Armstrong C, eds. *Myology*. 3rd Ed. Vol. 1, Chap. 2. New York: McGraw-Hill; 2004:45–65
30. Muller FL, Song W, Liu Y, et al. Absence of CuZn superoxide dismutase leads to elevated oxidative stress and acceleration of age-dependent skeletal muscle atrophy. Free Radic Biol Med 2006;40:1993–2004

31. Dobrowolny G, Aucello M, Rizzuto E, et al. Skeletal muscle is a primary target of SOD1G93A-mediated toxicity. Cell Metab 2008;8:425–36
32. Muller FL, Song W, Jang YC, et al. Denervation-induced skeletal muscle atrophy is associated with increased mitochondrial ROS production. Am J Physiol Regul Integr Comp Physiol 2007;293:R1159–68
33. Carlson BM. The denervated muscle: 45 Years later. Neurol Res 2008; 30:119–22
34. Midrio M. The denervated muscle: Facts and hypotheses. A historical review. Eur J Appl Physiol 2006;98:1–21
35. Gaillard S, Rock E, Vignon X, et al. 31P NMR and freeze fracture studies of sarcoplasmic reticulum membranes from normal and malignant hyperthermic pigs: Effect of halothane and dantrolene. Arch Biochem Biophys 1992;294:154–59
36. Renganathan M, Messi ML, Delbono O. Dihydropyridine receptor–ryanodine receptor uncoupling in aged skeletal muscle. J Membr Biol 1997;157:247–53
37. Fulle S, Protasi F, Di Tano G, et al. The contribution of reactive oxygen species to sarcopenia and muscle ageing. Exp Gerontol 2004;39:17–24
38. Fulle S, Belia S, Vecchiet J, et al. Modification of the functional capacity of sarcoplasmic reticulum membranes in patients suffering from chronic fatigue syndrome. Neuromuscul Disord 2003;13:479–84
39. Belia S, Pietrangelo T, Fulle S, et al. Sodium nitroprusside, a NO donor, modifies Ca^{2+} transport and mechanical properties in frog skeletal muscle. J Muscle Res Cell Motil 1998;19:865–76
40. Chomczynski P, Sacchi N. Single-step method of RNA isolation by acid guanidinium thiocyanate-phenol-chloroform extraction. Anal Biochem 1987;162:156–59
41. Adams L, Carlson BM, Henderson L, et al. Adaptation of nicotinic acetylcholine receptor, myogenin, and MRF4 gene expression to long-term muscle denervation. J Cell Biol 1995;131:1341–49
42. Dedkov AI, Kostrominova TY, Borisov AB, et al. Reparative myogenesis in long-term denervated skeletal muscles of adult rats results in a reduction of the satellite cell population. Anat Rec 2001;263: 139–54
43. Livak JK, Schmitten TD. Analysis of relative gene expression data using real-time quantitative PCR and the 2-ΔΔCT method. Methods 2001;25: 402–8
44. Pfaffl MW. A new mathematical model for relative quantification in real-time RT-PCR. Nucleic Acids Res 2001;29:e45
45. Paolini C, Quarta M, Nori A, et al. Reorganized stores and impaired calcium handling in skeletal muscle of mice lacking calsequestrin-1. J Physiol 2007;583:767–84
46. Esposito A, Germinario E, Zanin M, et al. Isoform switching in myofibrillar and excitation-contraction coupling proteins contributes to diminished contractile function in regenerating rat soleus muscle. J Appl Physiol 2007;102:1640–48
47. Midrio M, Danieli Betto D, Megighian A, et al. Early effects of denervation on sarcoplasmic reticulum properties of slow-twitch rat muscle fibers. Pflugers Arch 1997;434:398–405
48. Francini F, Stefani E. Decay of the slow calcium current in twitch muscle fibres of the frog is influenced by intracellular EGTA. J Gen Physiol 1989;94:953–69
49. Bencini C, Squecco R, Piperio C, et al. Effects of sphingosine 1-phosphate on intramembrane charge movement and L-type Ca^{2+} current in skeletal muscle fibres of mammal. J Muscle Res Cell Motil 2003;24:539–54
50. Francini F, Bencini C, Squecco R, et al. Separation of charge movement components in mammalian skeletal muscle fibres. J Physiol 2001;537: 45–56
51. Collins CA, Rojas E, Suarez-Isla BA. Fast charge movements in skeletal muscle fibres from *Rana temporaria*. J Physiol 1982;324: 319–45
52. Hnik P. Rate of denervation muscle atrophy. In: Gutmann E, ed. *The Denervated Muscle*. Prague: Publishing House of Czechoslovak Academy of Science; 1962:341–71
53. Adami N, Kern H, Mayr W, et al. Permanent denervation of rat tibialis anterior after bilateral sciatectomy: Determination of chronaxie by surface electrode stimulation during progression of atrophy up to one year. Basic Appl Myol 2007;17:237–43
54. Engel AG, Banker BQT. Ultrastructural changes in diseased muscle. In: Engel AG, Franzini-Armstrong C, eds. *Myology*. 3rd Ed. Vol. 1, chap. 31. New York: McGraw-Hill, 2004:749–87
55. Lapalombella R, Kern H, Adami N, et al. Persistence of regenerative myogenesis in spite of down-regulation of activity-dependent genes in long-term denervated rat muscle. Neurol Res 2008;30: 197–206
56. Borisov AB, Dedkov EI, Carlson BM. Interrelations of myogenic response, progressive atrophy of muscle fibres, and cell death in denervated skeletal muscle. Anat Rec 2001;264:203–18
57. Carraro U, Morale D, Mussini I, et al. Chronic denervation of rat diaphragm: Maintenance of fibre heterogeneity with associated increasing uniformity of myosin isoforms. J Cell Biol 1985;100:161–74
58. Mussini I, Favaro G, Carraro U. Maturation, dystrophic changes and the continuous production of fibers in skeletal muscle regenerating in the absence of nerve. J Neuropathol Exp Neurol 1987;46:315–31
59. Gutmann E. *The Denervated Muscle*. Prague: Publishing House of the Czechoslovak Academy of Science; 1962
60. Carraro U, Catani C, Dalla Libera L. Myosin light and heavy chains in rat gastrocnemius and diaphragm muscles after chronic denervation or reinnervation. Exp Neurol 1981;72:401–12
61. Takekura H, Kasuga N. Differential response of membrane systems involved in excitation-contraction coupling to early and later postnatal denervation in rat skeletal muscle. J Muscle Res Cell Motil 1999;20: 279–89
62. Germinario E, Esposito A, Midrio M, et al. Expression of sarco(endo) plasmic reticulum Ca(2+)-ATPase slow (SERCA2) isoform in regenerating rat soleus skeletal muscle depends on nerve impulses. Exp Physiol 2002;87:575–83
63. Ashley Z, Sutherland H, Lanmuller H, et al. Atrophy, but not necrosis, in rabbit skeletal muscle denervated for periods up to one year. Am J Physiol Cell Physiol 2007;292:C440–51
64. Biral D, Kern H, Adami N, et al. Atrophy-resistant fibers in permanent peripheral denervation of human skeletal muscle. Neurol Res 2008;30: 137–44
65. Squecco R, Bencini C, Piperio C, et al. L-type Ca^{2+} channel and ryanodine receptor cross-talk in frog skeletal muscle. J Physiol 2004; 555:137–52
66. Payne AM, Zheng Z, González E, et al. External Ca^{2+} dependent excitation–contraction coupling in a population of ageing mouse skeletal muscle fibres. J Physiol 2004;560:137–55
67. Hofer C, Forstner C, Mödlin M, et al. In vivo assessment of conduction velocity and refractory period of denervated muscle fibers. Artif Organs 2005;29:436–39
68. Stickler Y, Martinek J, Hofer C, et al. A finite element model of the electrically stimulated human thigh: Changes due to denervation and training. Artif Organs 2008;32:620–24
69. Favier FB, Henri Benoit H, Freyssenet D. Cellular and molecular events controlling skeletal muscle mass in response to altered use. Pflugers Arch 2008;456:587–600
70. Gerke V, Creutz CE, Moss SE. Annexins: Linking Ca^{2+} signalling to membrane dynamics. Nat Rev Mol Cell Biol 2005;6:449–61
71. Sandri M, Lin J, Handschin C, et al. PGC-1alpha protects skeletal muscle from atrophy by suppressing FoxO3 action and atrophy-specific gene transcription. Proc Natl Acad Sci U S A 2006;103:16260–65
72. Squecco R, Francini F, Kern H, et al. L-type Ca^{2+} channel mechanosensitivity in long-term denervated soleus muscle of the rat. Basic Appl Myol 2005;15:187–90
73. Squecco R, Kern H, Biral D, et al. Mechano-sensitivity of normal and long-term denervated soleus muscle of the rat. Neurol Res 2008;30:155–59
74. Billington L, Carlson BM. The recovery of long-term denervated rat muscles after marcaine treatment and grafting. J Neurol Sci 1996;144: 147–55
75. Schmalbruch H, Lewis DM. Dynamics of nuclei of muscle fibers and connective tissue cells in normal and denervated rat muscles. Muscle Nerve 2000;23:617–26
76. Carraro U, Rossini K, Zanin ME, et al. Induced myogenesis in long-term permanent denervation: Perspective role in functional electrical stimulation of denervated legs in humans. Basic Appl Myol 2002;12:53–64
77. Kern H. Funktionelle Elektrostimulation paraplegischer Patienten. Österr Z Phys Med 1995;5:1–79

